ISSN 0208-7774 TRIBOLOGIA 3/2018 p. 113–121

Arkadiusz RYCHLIK[*], Krzysztof LIGIER[*], Władysław KOZUBEL[**]

EFFECT OF HOLE-FORMING TECHNOLOGY ON THE DESTRUCTION OF MATERIAL DD11 USED TO MANUFACTURE WHEEL DISCS

WPŁYW TECHNOLOGII FORMOWANIA OTWORÓW NA DESTRUKCJĘ MATERIAŁU DD11 STOSOWANEGO NA TARCZE OBRĘCZY KOŁA

Key words: fatigue cracking, diagnostic signal, fatigue life, microscopic testing.

Abstract This study presents the results of comparative tests concerning the destruction process of specimens made of material DD11, for which different hole-forming technologies (i.e. drilling and piercing) were applied. For the analysis of cross-sectional properties of a specimen in the process of destruction, relative vibrations of the specimen's free end as a function of vibrations of a forcing mechanism (vibration inductor) were selected as the diagnostic signal. The tests were carried out on a test stand on which the destruction process of the material's cross-section was induced by the specimen's inertial force. Based on the conducted testing, it was found that the average value of cycles to damage a specimen with holes made using the drilling technique were more durable than the specimens with holes made using the piercing method.

Słowa kluczowe: pękanie zmęczeniowe, sygnał diagnostyczny, trwałość zmęczeniowa, badania mikroskopowe.

Streszczenie W pracy przedstawiono wyniki badań porównawczych procesu destrukcji próbek wykonanych z materiału DD11, dla których zastosowano różne technologie formowania otworów w postaci wiercenia i wykrawania. Do analizy właściwości przekroju próbki w procesie destrukcji jako sygnał diagnostycznych wybrano drgania względne swobodnego końca próbki w funkcji drgań mechanizmu wymuszającego (wzbudnika drgań). Badania przeprowadzono na oryginalnym stanowisku badawczym, w którym proces destrukcji przekroju materiału wywoływany jest przez siłę bezwładności próbki. Na podstawie przeprowadzonych badań można zauważyć, że próbki z otworami wykonanymi techniką wiercenia charakteryzują się większą trwałością w stosunku do próbek, w których otwory wykonano metodą wykrawania.

INTRODUCTION

The durability and strength of vehicle wheel rims are features which affect driving safety [**L. 1–3**]. Unfortunately, awareness of this fact can only be observed in certain sectors, such as aviation [**L. 4–7**], railway engineering [**L. 8–11**], or car racing. In the latter sector, wheel discs are always inspected visually prior to the installation, with magnetic and penetration methods applied in the case of doubt and, additionally, the total number of driving hours is monitored for particular rims. However, the nature of the problem has already been noted in "ordinary" road traffic. For example, the German Ministry of Transport has recognised that repaired wheels made of light alloys do not meet the initial strength parameters, and that their re-entry into service poses a hazard to traffic safety which is difficult to estimate.

[*] University of Warmia and Mazury in Olsztyn, Faculty of Technical Sciences, ul. M. Oczapowskiego 11, 10-736 Olsztyn, Poland.
[**] POLKAR Warmia Sp. z o.o. ul. Elbląska 3, 14-420 Mlynary, Poland.

However, the existing written regulations concerning tests on wheel rims are not mandatory for their manufacturers, and only concern the testing and control of new types and designs of wheel rims which, prior to being introduced to industrial series production, are subjected to a variety of strength and type-approval tests. In the very process of wheel rim manufacturing, however, it is difficult, at any of its stages, to identify a comprehensive, reliable system of quality control providing a quick answer to the question concerning the quality of the batch currently being manufactured.

Despite correctly designed rims and their manufacturers' efforts to maintain manufacturing and competence standards, cases of premature fatigue wear do occur. Typical situations resulting in fatigue damage to a wheel rim during the operation can be divided into three groups [**L. 12**]:

– Damage to a wheel disc caused by frictional fatigue within the area of connection with the rim;
– Propagation of cracks from the area of a ventilation hole or disc mounting holes to the hub of the vehicle; and,
– Fatigue wear of welds – the connection of the disc with the circular blank [**L. 13**].

The testing concerned the degree of impact of particular operations on the fatigue strength, with particular emphasis on the relationships between the surface hardness and the stresses induced within the wheel disc. It was demonstrated that this is the first stage of production, i.e. the so-called first pressing of the wheel disc that contributes the most to the reduction in fatigue life.

According to the authors, the phenomenon of a reduction in fatigue life during the manufacturing of wheel discs [**L. 13**] is associated with the "cold" operation of sheet-metal forming that results in the generation of residual tensile stresses (as opposed to, for example, cold rolling operations resulting in compressive stresses that improve the fatigue properties of the material). The considerable increase in the value of residual stresses while shifting from the "pressing" stage to the "piercing" stage is probably due to a reduction in the volume of the material (in which holes are made) and to the development of a new energy equilibrium system. This phenomenon could only be explained after conducting an analysis of the micro-structure, which revealed the precipitation of carbonitrides at the boundaries of grains as well as changes in martensite grains.

When further examining this issue [**L. 14**], the mean stress models of Soderberg, Goodman, and Gerber were applied in order to predict the fatigue life of a wheel rim. The Gerber model, which emphasised the effect of the wheel disc manufacturing process on residual stresses (and thus the fatigue properties of the rim) was considered to be the most useful.

In the study [**L. 15**], the authors applied the Taguchi method and the analysis of variance to determine significant factors contributing to the development of weld cracks in the process of wheel rim manufacturing.

In turn, the study [**L. 16**] investigated the phenomenon of premature cracking of wheel rims in the group of light commercial vehicles. It was found that cracks initiated within the area of ventilation holes and mounting holes in the wheel disc. Mechanical properties and chemical composition of the sheet metal used to manufacture rims, both the damaged and resistant to damage, were similar; however, differences were noted in the micro-structure and hardness of the edges of ventilation holes and mounting holes of the wheel disc. In addition, the presence of burrs on the perimeter of the holes as well as a number of micro-cracks at the base of these burrs were also noted. The hardness of the material in these locations was much greater than that of the native material. This was caused by the production process during which the areas around the holes were subjected to excessive deformations and hardening. This resulted in the formation of small cracks within these areas, which subsequently developed due to fatigue during operation. These holes are pierced during production, and the gap between the die and the piercing die punch was incorrect, most probably due to their wear. In the production process, the burrs were not removed and the edges were hardened. In turn, the increase in hardness in these areas resulted in a decrease in ductility and a tendency to form cracks.

An analysis of the causes of premature damage to the wheel rim during torsional bending resistance tests was conducted in the study [**L. 17**]. The authors concluded the following:

– Damage mainly occurs within the areas of the holes in the wheel disc; on the other hand, no fatigue cracks were noted on the wheel rim and on the welded joints between the disc and the rim. Therefore, the process of deep drawing of a wheel disc (i.e. the formation of the final form of the wheel disc) reduces the fatigue life and increases stresses due to a reduction in the thickness of the material of the disc and to residual tensile stresses generated as a result of disc pressing.
– Fatigue cracks have appeared on the perimeter of the disc and their lengths are almost identical. Therefore, this is not a matter of defects in material or the quality of the surface, but rather of the mechanical fatigue of the material during tests.
– In addition, fatigue cracks were observed on the disc surface, and they are more likely related to the quality of the disc surface, changes in thickness and residual tensile stresses.

In the process of wheel rim manufacturing, it is of extreme importance to develop a comprehensive, reliable system of quality control providing a quick answer to the question concerning the quality of the batch being currently manufactured. The publication [**L. 18**] suggests a system of rim quality control at selected stages of production with the application of accelerated

fatigue testing. The suggested system involves an inspection at the stage of material delivery (preliminary testing – inspection of the delivery), welding (quality tests on welded joints, i.e. specimens), and the pre-shipment inspection (testing on the finished product). The preliminary testing is aimed at the determination of whether the purchased material (sheet metal) meets the fatigue strength requirements laid out in standards and certificates, i.e. whether the material used for production would not be subject to fatigue failure prior to the performance of a specified number of load cycles. The tests carried out during the production process concern the verification of fatigue life of the samples of welds made during the technological process. Welded joints can be made both manually and using a welding robot. The test is performed to assess the durability and quality of the welded joint, but it can also be used to verify the welder's competence. The pre-shipment test involves destructive testing on the rim. Similarly to the tests during the production process, it is aimed at assessing the durability of welded joints; however, specimens are collected from a finished product.

The aim of the experimental tests carried out in the study [**L. 19**] was to identify the diagnostic signal and to determine its features in order to identify irregularities in the welded joints between the wheel disc and the rim using a vibroacoustic signal. Analyses of damage to wheel discs revealed the occurrence of defects of joints in the form of not full or incomplete penetration of the joint between the disc and the rim, resulting in the lack of connection between one or more wheel disc spokes and the rim. For new rims, this is an effect of improper parameters of the welding process during their production. A similar phenomenon can also be observed for wheel discs with specific kilometrages. The loss of the connection between the disc spokes and the rim may be caused by a fatigue or overload crack, and through a change in the structure properties as an effect of other phenomena, e.g., corrosion of the weld or of the material of the wheel disc or rim, identified using a vibration signal. The study was further extended by studies [**L. 20–21**].

The problem of identification of structural damages based on vibrations has been addressed by numerous authors [**L. 22–31**]. In this approach, the parameters of vibrations of objects are specified, and the identification of structural damage is a function of the change in the structural properties of the object such as the rigidity and weight. The presence of damage affects both the response of a vibration signal and the dynamic properties of a particular structure, which include natural frequencies, shapes, and indicators of the damping mode. These properties are used as indicators of damage to the tested structure. The detection of structural damage at an early stage enables timely maintenance and repairs extending the system's life.

In order to ensure safety and structural reliability, it is necessary to perform long-, medium- and short-term monitoring of the technical condition of the structure in the production and operation of a wheel rim. One of the basic dynamic properties of a structure is its rigidity, a change in which may lead to changes in the pattern of the course of changes in natural frequencies and to an increase in the damping factor.

Based on the analysis of warranty and post-warranty complaints conducted at the enterprise Polkar Warmia, a rather considerable percentage of damage to wheel rims was noted within the areas around the mounting holes, as presented in **Fig. 1**. Some of them probably resulted from the improper process of wheel operation, yet a significant percentage of the damage was not associated with it, as indicated by a visual inspection. In the technology of wheel disc manufacturing at the enterprise Polkar Warmia, the process of hole piercing in the semi-finished wheel disc is applied. Therefore, as part of the research work carried out, an attempt was made to determine the causes of the formation of such defects and to specify measures to prevent them.

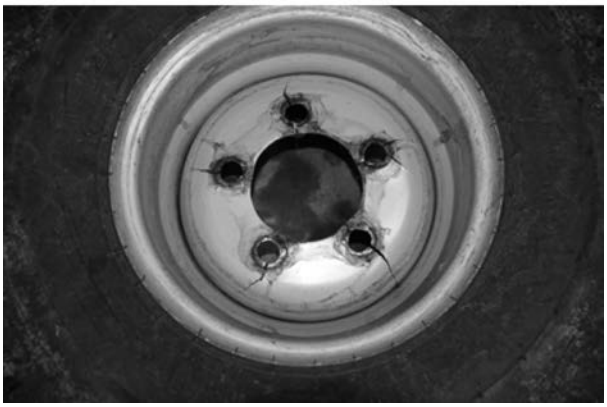

Fig. 1. A view of a wheel rim with cracks formed on the mounting holes in the wheel disc

Rys. 1. Widok obręczy koła z pęknięciami powstałymi na otworach montażowych tarczy koła

This study presents an attempt to assess the effects of the technology of making holes in a wheel disc on its fatigue strength. An inertial fatigue-testing machine was used as a test stand, and a vibration signal was used to identify a loss in the continuity of the specimen structure (cracks). In order to limit the duration and costs of the conducted study, it was decided to test material specimens and not complete wheel rims.

TEST STAND

The laboratory testing was conducted on an inertial test stand designed for accelerated fatigue tests, presented in **Fig. 2**. The test stand comprises a reciprocating motion generator (crankshaft) to which a plate with a holder in the form of a vice is attached, and the specimen is clamped in a vice and the whole unit is moved on linear bearings. The amplitude of displacements of the

specimen holder in this particular case is 1 mm (throw of the crankshaft of 0.5 mm). A detailed description of the design and operation of the test stand can be found in the study [**L. 20–21**].

The test stand enables the setting of a specimen in oscillatory motion with a specified frequency and a constant displacement amplitude. Due to the oscillatory motion and the one-sided clamping of the specimen, the resulting inertial forces cause its elastic strains.

For the identification of the dynamic parameters of the system, two ICP-100 piezoelectric vibration acceleration sensors and a driving motor rotational speed sensor were used. One of the vibration sensors at the test stand identifies the acceleration of the specimen's free end, while another identifies the acceleration of the mounting holder of the tested specimen. For the recording, visualisation, and analysis of the obtained data, a multi-channel KSD-400 recorder based on a NI 6343 card controlled by LabVIEW was used.

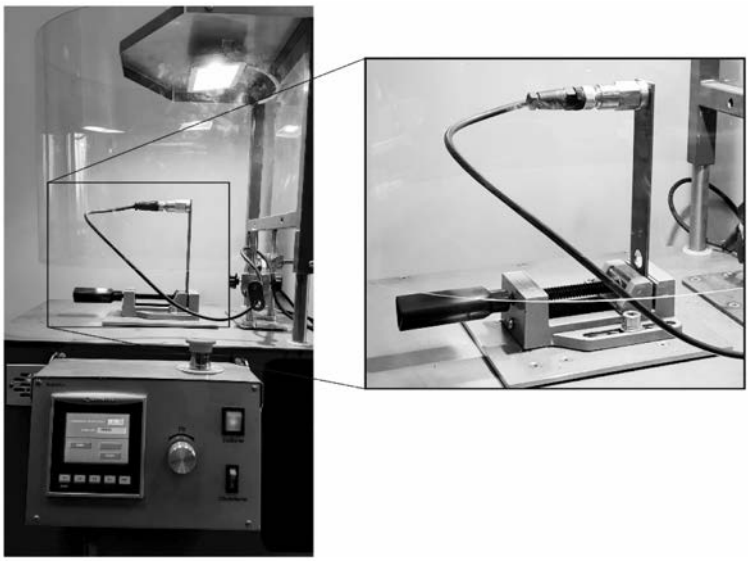

Fig. 2. A general view of a test stand designed for accelerated durability testing and of the method of test specimen mounting

Rys. 2. Widok ogólny stanowiska do przyśpieszonych badań trwałościowych oraz sposobu montażu próbki badawczej

A visual inspection of specimens was performed using microscopic observations using the light microscopy method.

TEST OBJECT

The test object was a flat specimen with dimensions of 180x35 mm and a thickness of 3 mm made of DD11 sheet metal (R_e=254 [MPa], R_m=350 [MPa]). The test specimens were cut out from sheet metal strips using a shearing machine along the rolling direction. Then, in the first group of specimens (G1), holes (ø 15.8 mm) were made using the drilling method, while in the second group of specimens (G2), holes (ø 15.8 mm) were pierced using tools and devices used in the production process at the Polkar Warmia enterprise.

TESTING PROCEDURE AND TEST RESULTS

The laboratory tests involved the determination of a durability curve for the test specimens for the same weights imposing the load on the specimen (exciting force) but for different technologies of making holes in them. To shorten the duration of testing, a frequency of the specimen's motion similar to resonance frequency of the test specimens was adopted.

Parameters of the conducted research tests are listed in **Table 1**.

Average computational stresses in the specimen's notch cross-section were determined using an analytical method based on the geometrical dimensions of the specimen, the location of mounting of the measurement sensor, and the weights and dynamics of the free motion of the specimen's free end during the testing.

The number of specimens for each measurement series was established to be 10. To identify the specimen's cross-section destruction process, relative vibrations recorded by the lower sensor (located on the vice base) as a function of the value of vibrations recorded by the upper sensor located at the specimen's free end were used.

Table 1. Technical and operational parameters were realised during laboratory tests on DD11 specimens
Tabela 1. Parametry techniczno-eksploatacyjne realizowane podczas badań laboratoryjnych próbek DD11

Item	Distinguishing attribute of a feature	Measurement series	
		Drilled specimens G1	Pierced specimens G2
1	Weight imposing a load on the specimen (including the sensor's weight) [g]	285	285
2	Frequency of proper vibrations of the specimen with the weight [Hz]	26	26
3	Excitation frequency [Hz]	28	28
4	Computational stresses in the cross-section of the specimen [MPa]	172	172

Assuming that the amplitude of acceleration from the lower measurement point (A_{Down}) is a certain function α of time (t), frequency (f) and the amplitude (S) of the excitation force, which can be described using the formula $A_{Down} = \alpha(t, f, S)$, the acceleration amplitude from the upper measurement point (A_{UP}) is a certain function β of elasticity (k), damping (c), the specimen's weight (m), and length (l) described using the formula $A_{UP} = \beta(A_{Down}, k, c, m, l)$. Therefore, each change in the properties of the structure of the specimen's cross-section must be identified by a change in the specimen's free end's vibration acceleration amplitude in relation to the amplitude of acceleration forcing the motion of the vibratory system.

Therefore, the ratio of the maximum amplitudes of accelerations of vibrations identified by the measurement sensors was adopted as the diagnostic signal measure, and the obtained coefficient was described as the vibration amplitude flattening coefficient. The value of the coefficient at a level $A \geq 1.5$ determined in accordance with the formula below was adopted as the limit value determining the start of the destruction process.

$$A = \frac{A_{UP(max)}}{A_{Down(max)}} \geq 1.5 \quad (1)$$

where

$A_{UP(max)}$ – max. value of the amplitude of vibration acceleration, read from the time course by the upper vibration sensor;

$A_{Down(max)}$ – max. value of the amplitude of vibration acceleration, read from the time course by the lower vibration sensor (vice base).

The limit value of flattening coefficient A was determined experimentally for the tested model and type of test specimen. The frequency of the readout of vibration amplitudes for the identification of vibration amplitude flattening coefficient was 10 Hz.

The testing process was interrupted automatically by the test stand control system following the identification of the limit value of the relative vibration flattening coefficient.

At the next stage of testing, the specimen was analysed visually. All specimens were subjected to microscopic testing.

Fig. 3 shows the course of the change in the number of the specimen's test cycles in the function of stresses in the notch cross section for a specimen with a drilled (G1) and pierced (G2) hole at a vibration excitation frequency of 28 Hz. The diagram distinguishes mean values as well as max. and min. values for each test series.

In analysing the obtained results for damage-tested DD11 sheet metal for various hole-making technologies, it was noted that the specimens with drilled holes were characterised by a higher average number of cycles before the damage occurred. The conducted tests demonstrated that the specimens with drilled holes had a durability greater by approx. 28% and expressed by the average number of cycles before the damage occurs, compared to the specimens in which holes were pierced.

Fig. 4 presents examples of relative vibration trajectories recorded by the upper sensor as a function of the value of relative vibrations recorded by the lower sensor at various stages of the experiment. The results were presented for specimen G1-3, with the vibration amplitude flattening coefficient being distinguished. Each diagram of the relative vibrations represents a one-second "shot" of the experiment.

Up to approx. 6,000 test cycles, the shape of the relative vibration diagram recorded by the upper vibration sensor as a function of vibrations recorded by the lower sensor remained unchanged – compared to the first shape (320 cycles) – **Fig. 4**. From this point on, noticeable changes in the shape and size appear in subsequent images of the forms of relative vibrations. The flattening coefficient behaves in a similar manner, as during the initial period it oscillates within a range of 1.29, and then, close to approx. 6 000 cycles, it systematically increases up to a value of approx. 1.33 (this is due to the hardening of the specimen's cross-section). During the initiation of single cracks in the specimen's cross-section structure, the coefficient increases rapidly. When the experiment is continued, the coefficient begins to increase systematically. Monitoring the flattening coefficient and its graphic interpretation provides a clear and reliable method of identifying single cracks in the specimen's cross-section.

During the preliminary testing, tests were also carried out to determine the number of cycles from the moment of identifying damage to the cross-section

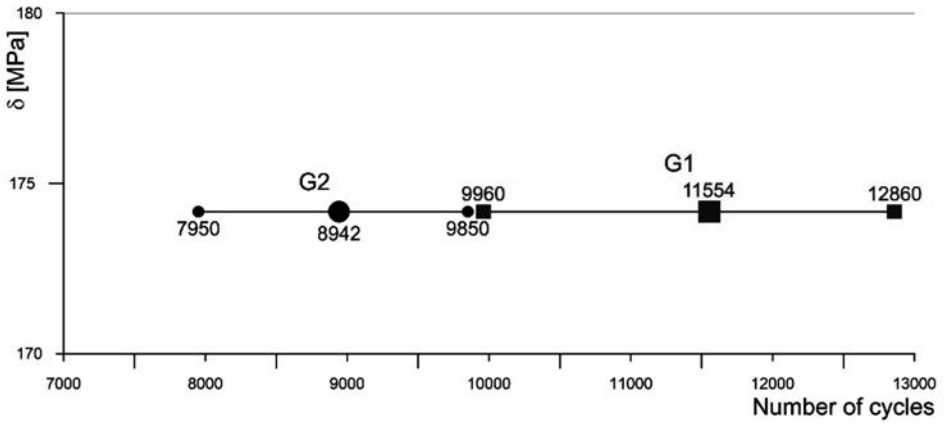

Fig. 3. The course of the change in the number of test cycles for a drilled (G1) and pierced (G2) specimen operated within the range of proper vibrations (28 Hz), with the average, max and min values distinguished for each measurement series

Rys. 3. Przebieg zmiany liczy cykli badawczych próbki wierconej (G1) i wykrawanej (G2) przy eksploatacji jej w zakresie częstotliwości drgań własnych (28 Hz) z wyróżnieniem wartości średniej, maks. i min. dla każdej z serii pomiarowych

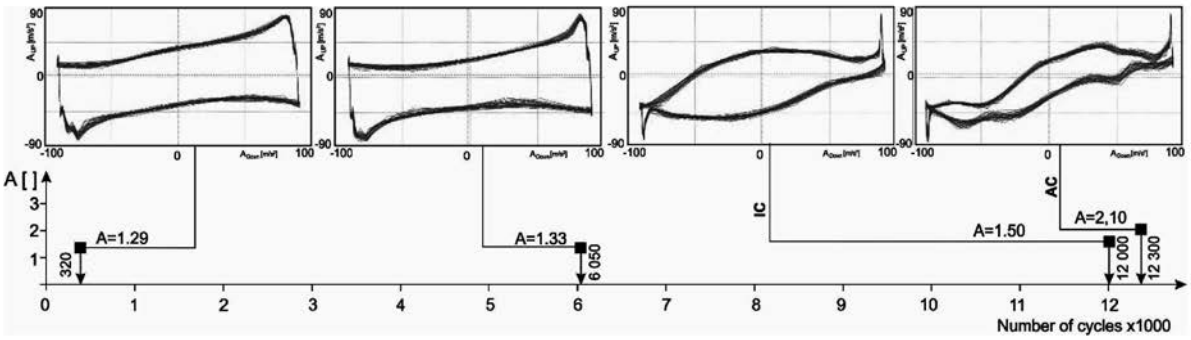

Fig. 4. Sequences of the diagrams of relative vibrations and the amplitude flattening coefficient for drilled specimen No G1-3 at various stages of the experiment, IC – the initiation of cracking of the specimen's cross-section, AC – advanced crack of the cross-section

Rys. 4. Sekwencje wykresów drgań względnych oraz współczynnika spłaszczenia amplitud próbki wierconej nr G1-3 w różnych fazach eksperymentu, IC – początek pękania przekroju próbki (initiation of cracking), AC – zaawansowane pęknięcie przekroju (advanced crack)

using the vibroacoustic method to the number of cycles in which the specimen's free part will separate from the part mounted in the holder. These tests revealed that the average number of cycles is from 10% to 40% of the average number of cycles determined using the vibroacoustic method, with this number of cycles increasing for the lower value of stresses in the specimen's cross-section.

In all test specimens where the initiation of the cracking process was identified using the vibroacoustic analysis by the relative vibration method, the occurrence of a crack was confirmed by an analysis of the condition of the specimen surface using microscopic methods.

A visual analysis of the condition of specimen surface

The specimens for which the testing was interrupted at the stage of the initiation of the cracking process were analysed visually.

The surface of the specimens near the edge of the hole and the internal surface of the hole were visually inspected.

Figure 5 shows a micro-image of the surface of specimens pierced (a) and drilled (b) within the edge area of the hole. In both specimens, a crack is visible which initiates at the edge of the hole and propagates perpendicularly to the specimen's axis.

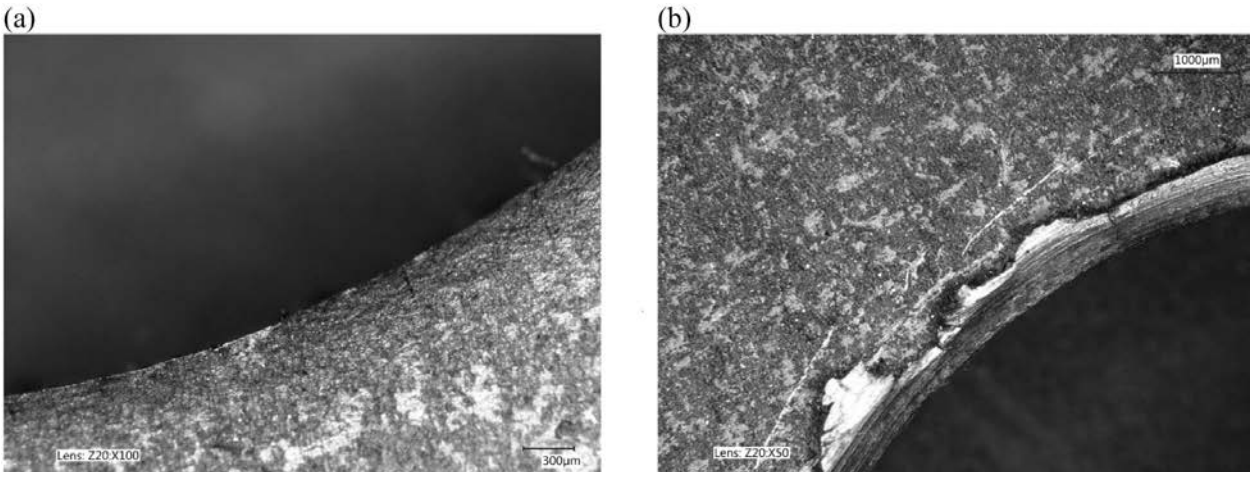

Fig. 5. A view of the specimen surface with a hole pierced (a) and drilled (b) at the stage of cracking initiation
Rys. 5. Widok powierzchni próbki z otworem wykrawanym (a) i wierconym (b) w fazie początku pękania

In order to determine the location of the initiation of the cracking of specimens with pierced holes, the internal surfaces of holes were visually inspected. A view of the internal surface of a pierced specimen is presented in **Fig. 6**. On the internal surface of the hole, two areas associated with the hole-making technology can be observed. The area of material shearing at the first stage of piercing, where signs of the action of a punch

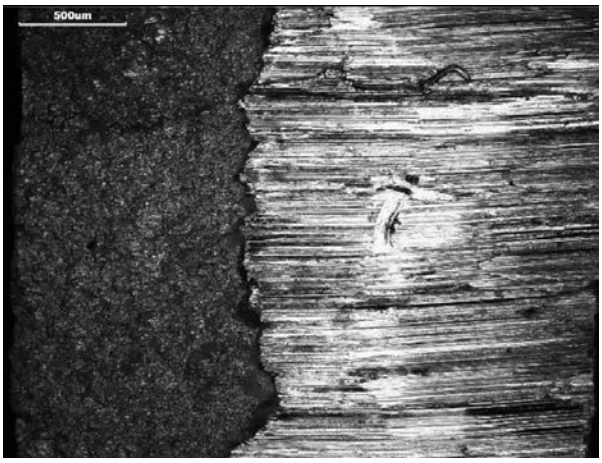

Fig. 6. A view of the internal surface of a pierced hole
Rys. 6. Widok wewnętrznej powierzchni otworu wykrawanego

directed in accordance with its operating motion can be clearly seen, along with the area where the specimen's material has been torn off and pushed out of the hole being made. In turn, this area is characterised by the lack of surface orientation and by the presence of breaches. All of the observed cracks were initiated in the area where the material is torn off and pushed out. These cracks are initiated in these deep breaches (**Fig. 7**) and in locations where the material has been torn off (**Figs. 8** and **9**).

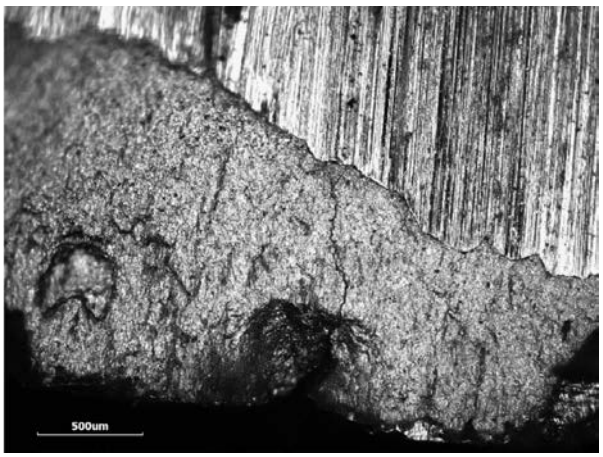

Fig. 7. The initiation of a crack in a deep breach formed within the area where the material has been pushed out and torn off
Rys. 7. Inicjacja pęknięcia w głębokiej wyrwie powstałej w obszarze spychania i odrywania materiału

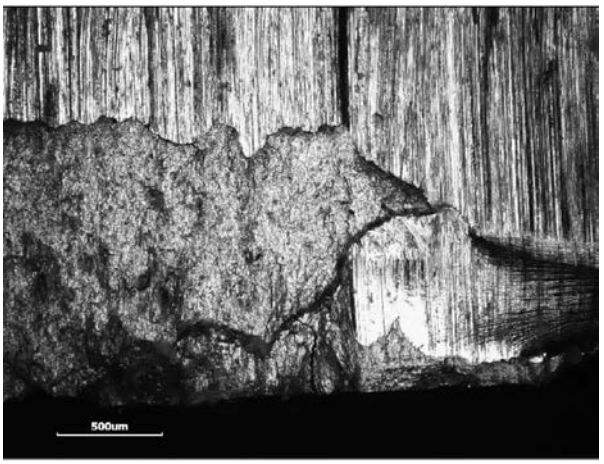

Fig. 8. The initiation of a crack in the location where the material has been peeled off
Rys. 8. Inicjacja pęknięcia w miejscu oderwania materiału

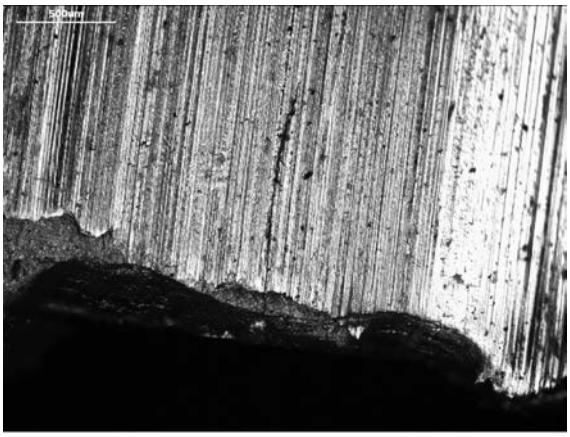

Fig. 9. Crack propagation from the initiation area to the material shearing area

Rys. 9. Propagacja pęknięcia z obszaru inicjacji do obszaru ścinania materiału

The technology of hole-making through piercing results in sharp burrs and material flashes. Failure to remove these processing residues promotes crack initiation, from where they spread deep into the material, which is presented in **Fig. 10**. The initiation of a crack always occurs near the edge of a hole on the hole-making tool exit side.

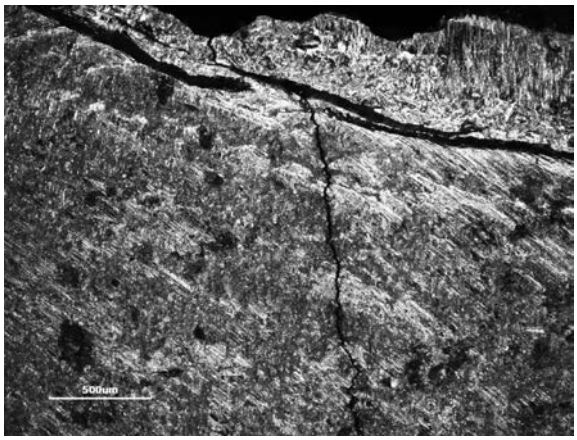

Fig. 10. A crack initiated on the unremoved burr after piercing the hole

Rys. 10. Pęknięcie zainicjowane na nieusuniętej wypływce materiału po wykrawaniu otworu

CONCLUSIONS

Based on the conducted testing, the following conclusions can be formulated:

- An analysis of the damage curves for test specimens reveals that the specimens with drilled holes are characterised by greater durability than the specimens with pierced holes. The study demonstrated that the average fatigue strength of the specimens in which holes were drilled is greater by approx. 28% than that of the specimens with pierced holes.
- An analysis of the available literature, as well as the conducted study, indicate that, in this case, the lower fatigue strength of the pierced holes, compared to the drilled holes, is caused by the production process during which the areas around the holes were subjected to excessively large deformations, and thus hardening. Consequently, this resulted in the formation of small cracks near the edges of pierced holes, which subsequently developed due to the fatigue during the tests on the specimen or the operation of wheel rims.
- These phenomena are caused by an excessively large gap between the die and the piercing die punch, which, during the piercing of discs, forms burrs and damage to the structure of the hole edges as well as their local hardening, which increases the tendency to the formation of cracks.
- On the surface of pierced holes, two zones can be distinguished: the material shearing zone characterised by the surface orientation, and the zone where the material is pushed and torn off, which is characterised by a lack of orientation.
- A microscopic analysis of the surfaces of holes indicated that the initiation of the fatigue crack occurs within the zone where the material is pushed out and torn off, and it is located in the breaches on the edge of a hole on the punch exit side.

This research study was carried out as part of the project NCBR No POIR.01.01.01-00-1746/15 by POLKAR Warmia Sp. z o.o.

REFERENCES

1. Firat M., et al.: Numerical modelling and simulation of wheel radial fatigue tests. Engineering Failure Analysis 16.5 (2009)
2. Elvik R., et al., eds.: The handbook of road safety measures. Emerald Group Publishing Limited, 2009.
3. Burdzik R., Sadowski A.: Przegląd metod badania kół tarczowych w pojazdach samochodowych. Prace Naukowe Politechniki Warszawskiej. Z. 112 Transport. 2016.
4. Dreher R.C.: An Airborne Indicator for Measuring Vertical Velocity of Airplanes at Wheel Contact. National Advisory Committee for Aeronautics, 1953.

5. Hohmann R. et al.: Aircraft wheel testing with machine-cooled HTS SQUID gradiometer system. IEEE transactions on applied superconductivity 9.2 (1999), pp. 3801–3804.
6. Kosec B., Kovacic G., Kosec L.: Fatigue cracking of an aircraft wheel. Engineering Failure Analysis 9.5 (2002), pp. 603–609.
7. Kappes W., et al.: Non-destructive testing of wheel-sets as a contribution to safety of rail traffic. CORENDE 2000 Proceedings (2000).
8. Kappes W., et al.: Application of new front-end electronics for non-destructive testing of railroad wheel sets. Insight-Non-Destructive Testing and Condition Monitoring 49.6 (2007), pp. 345–349.
9. Joshi Anjali, Mats PE Heimdahl: Model-based safety analysis of simulink models using SCADE design verifier. International Conference on Computer Safety, Reliability, and Security. Springer Berlin Heidelberg, 2005.
10. Mutton P.J., Lynch M.R.: Improving the safety of railway wheels through non-destructive measurement of residual stresses. CORE 2004: New Horizons for Rail (2004): 25.
11. Diener M., Ghidini A.: Reliability and safety in railway products: fracture mechanics on railway solid wheels; a challenge for appliers and producers. Lucchini RS, 2008.
12. Carboni M., Beretta S., Finzi A.: Defects and in-service fatigue life of truck wheels, Engineering Failure Analysis 10 (2003), pp. 45–57.
13. McGrath P.J., et al.: Effects of forming process on fatigue performance of wheel centre discs. ECF13, San Sebastian 2000. 2013.
14. McGrath P.J.: An investigation of residual stresses induced by forming processes on the fatigue resistance of automotive wheels. (2001).
15. Prajapati D.R., Satsangi P., Daman Vir Singh Cheema: Taguchi approach to optimize the bad fusion defect of wheel rim industry: A case study. International Journal of Management, IT and Engineering 3.9 (2013): 121.
16. Wali M., Ahnaf Usman Zillohu: Failure of Wheels Due to Improper Manufacturing Process. Journal of failure analysis and prevention 10.5 (2010), pp. 387–392.
17. Zhanguang, Zheng, Shuai Yuan, Teng Sun, Shuqin Pan, Fractographic study of fatigue cracks in a steel car wheel, Engineering Failure Analysis 47 (2015), pp. 199–207.
18. Drożyner P., Rychlik A.: The use of fatigue tests in the manufacture of automotive steel wheels. Materials Science and Engineering 145 (2016), DOI:10.1088/1757-899X/145/2/022033.
19. Rychlik A., Kozubel W.: A method of fatigue strength testing of wheel rim fragments at the production process stage. Journal of KONES Powertrain and Transport, Vol. 23, No. 1 2016, pp. 289–296. ISSN: 1231-4005 e-ISSN: 2354-0133 DOI: 10.5604/12314005.1213506.
20. Rychlik A., Ligier K.: Fatigue crack detection method using analysis of vibration signal. Technical Sciences 20 (1)2017.
21. Rychlik A., Ligier K., Kozubel W.: Identification of fatigue damage of metal sheet made of material DD11 from an analysis of a vibration signal. Tribologia 6/2017, pp. 87–93.
22. Białkowski P., Krężel B.: Early detection of cracks in rear suspension beam with the use of time domain estimates of vibration during the fatigue testing. DIAGNOSTYKA, Vol. 16, No. 4 (2015), pp. 55–62.
23. Broda D., Klepka A., Staszewski W.J., Scarpa F.: Nonlinear Acoustics in Non-destructive Testing – from Theory to Experimental Application. Key Engineering Materials. 2014, Vol. 588, pp. 192–201.
24. Byung Kwan Oh, Se Woon Choi, Hyo Seon Park1: Damage Detection Technique for Cold-Formed Steel Beam Structure Based on NSGA-II. Shock and Vibration. Volume 2015 (2015), Article ID 354564.
25. Jassim Z.A., Ali N.N., Mustapha F., Abdul Jalil N.A.: A review on the vibration analysis for a damage occurrence of a cantilever beam. Engineering Failure Analysis 31 (2013), pp. 442–461.
26. Klepka A., Pieczonka L., Staszewski W.J., Aymerich F.: Impact damage detection in laminated composites by non-linear vibro-acoustic wave modulations. Composites: Part B 65 (2014), pp. 99–108.
27. Qingsong Xu: Impact detection and location for a plate structure using least squares support vector machines. Structural Health Monitoring 2014, Vol. 13(1), pp. 5–18.
28. Tao Jinniu, Feng Yongming, Tang Kezhong: Fatigue crack detection for a structural hotspot. Journal of Measurements in Engineering, Vol. 2, Issue 1, 2014, pp. 49–56.
29. Trochidis A., Hadjileontiadis L., Zacharias K.: Analysis of vibroacoustic modulations for crack detection: A Time-Frequency Approach Based on Zhao-Atlas-Marks Distribution. Hindawi Publishing Corporation, Shock and Vibration, Volume 2014, Article ID 102157.
30. Trojniar T., Klepka A., Pieczonka L., Staszewski W.J.: Fatigue crack detection using nonlinear vibro-acoustic cross-modulations based on the Luxemburg-Gorky effect. Health Monitoring of Structural and Biological Systems (2014).